JOURNAL OF Applied Polymer SCIENCE

Thermal and Mechanical Properties of Homogeneous Ternary Nanocomposites of Regioregular Poly(3-hexylthiophene)-Wrapped Multiwalled Carbon Nanotube Dispersed in Thermoplastic Polyurethane: Dynamic- and Thermomechanical Analysis

Suparna Saha,[1] Uttam Saha,[2] Jyoti Prakash Singh,[2] Thako Hari Goswami[2]

[1]Department of Polymer Science & Technology, University of Calcutta, Kolkata 700009, India

[2]Electronics and Smart Materials Division, Defence Materials and Stores Research and Development Establishment, Kanpur 208013, India

Correspondence to: T. H. Goswami (E-mail: thgoswami@yahoo.co.uk)

ABSTRACT: An interesting correlation between initial loading and nature of wrapping of regioregular poly(3-hexylthiophene) (rrP3HT) on multiwalled carbon nanotube and their combined effect on dynamic- and thermomechanical properties in ternary system (thermoplastic polyurethane as matrix) is highlighted. Wrapping of rrP3HT on carbon nanotube (CNT) makes the hexyl side chains thermally nonequivalent and composites more stable. Dynamic- and thermomechanical analysis ascertained the miscibility (single $T_g = -40°C$), large mechanical reinforcement, and improved storage modulus of nanocomposites in the presence of CNT compared to its blends. Two breaks at ~ -100 and $\sim -40°C$ for TPU-P3HT composites (PHs) and TPU-P3HT-MWCNT composites (PHCs) in the loss modulus vs. temperature plot indicates two different types of transitions in P3HT chains. Dimensional stability by expansion probe technique measures low coefficient of thermal expansion of PHCs compared to its blends. Softening property by penetration probe technique suggests that 2.5 wt % loading of P3HT exhibits lowest degree of penetration compared to other nanocomposites. © 2012 Wiley Periodicals, Inc. J. Appl. Polym. Sci. 000: 000–000, 2012

KEYWORDS: composites; conducting polymers; differential scanning calorimetry (DSC); glass transition; nanotubes; graphene and fullerenes

Received 31 May 2012; accepted 26 July 2012; published online
DOI: 10.1002/app.38397

INTRODUCTION

Blending is an attractive route to improve material properties and also enhances possibility for expanding the range of material's applications. Thermoplastic polyurethane (TPU) is an interesting class of material and blending with polythiophenes/carbon nanotubes (CNTs) enables combination with the mechanical property of TPU and the transport and optical properties of conjugated polymers.[1,2] Polyurethane has significant industrial importance owing to its wide range of applications as coatings, sealants, trans-dermal patches, and in catheters.[3] Among the shape memory polymers (SMPs), TPUs have received increasing attention because of their excellent shape recovery characteristics. They exhibit good elasticity and strength, depending on the nature and amount of polyol, isocyanates, and chain extender.[4,5] Thermoresponsive SMPs are temperature-sensitive, functional polymers and often observed in the case of block or segmented copolymers. These polymers basically consist of two phases: a frozen phase (or fixed phase) and a reversible switching phase. The fixed phase (hard segment) arises either from entanglement of polymeric chains or from chemical and physical crosslinking. The reversible phase constitutes the soft segment. Desmopan (DP 9380A), the commercial grade TPU, is extensively studied for its excellent shape memory effects and finds broad applications in temperature-sensing elements. Also, a low-cost chemiresistive sensor[6] can be developed by imparting transport and optical properties of fluorescent conductive material to the nonconductive matrix.[7] Recently, polyurethane–CNT composites received substantial attention[3] and composite nanofibers and films were made from the solution-mixed homogeneous dispersions of single-walled nanotubes into a PU matrix.[3,8] Novel remote actuation has been demonstrated by incorporating CNTs into the traditional thermoplastic elastomer.

Highly conductive π-conjugated polymers create an opportunity to be used as promising low-cost alternatives to conventional

Additional Supporting Information may be found in the online version of this article.

© 2012 Wiley Periodicals, Inc.

light-emitting diodes, photovoltaic cells, and disposable electronic chips.[9,10] Among its members, poly(alkylthiophenes), in particular, regioregular poly(3-hexylthiophene) (rrP3HT)[11,12] has been the focus of great attention owing to its relative high chemical stability[13] in ambient conditions, excellent solubility in variety of solvents, and high conductivity.[14,15] Conductivity of this polymer depends on head–tail regioregularity of the chain and is highly selective to processing condition; the higher the regioregularity, the higher is the conductivity.[16,17] Certainly, the first important consideration when tailoring the electronic properties of rrP3HT is to determine the effect of regioregularity and molar mass of the polymers.

Considerable research interest has also been focussed on CNTs owing to their unique physical and mechanical (high modulus) properties[18] and high electrical and thermal conductivity.[19,20] Inclusion of CNTs into a polymer matrix holds the potential to improve the host material's mechanical, electrical, and thermal properties by orders of magnitude well above the performance possible with traditional fillers. A better understanding of the interaction between polymers and nanotube is still a critical issue and a correct knowledge of these interactions will allow optimization of polymer–nanotube compositions to make composite materials with improved performances. Key issues for producing superior CNT nanocomposites are (i) to determine appropriate percentage weight ratio of conducting polymers to CNT to obtain uniform wrapping; (ii) homogeneous dispersion of wrapped CNTs in polymeric matrix; and (iii) strong interfacial interaction so as to effect efficient load transfer from polymeric matrix to CNTs. In general, CNTs are difficult to process owing to their insolubility in most solvents. One strategy to overcome this difficulty is to wrap the CNT with polymer which renders them soluble in common solvents.[21] Solution casting and melt-mixing techniques[22] have reached a stage suitable for the fabrication of polymer–nanotube composites for high performance and multifunctional components. Recently, direct polymerization of monomers in a CNT-dispersed medium has received great attention as a route to prepare polymer-wrapped CNTs.[23,24]

In this study, dynamic- and thermomechanical properties of TPU–rrP3HT blends (PHs) prepared at different concentrations of P3HT are investigated. Thermal effect of CNT (fixed concentration, 0.5 wt %) on PH blends is compared by studying thermal properties of TPU–P3HT–CNT ternary nanocomposites (PHCs) and binary PH blends. dynamic mechanical analysis (DMA) and thermomechanical analysis (TMA) studies are able to provide valuable information regarding storage modulus, loss modulus, damping properties (tan δ) and dimensional stability of materials. A relationship between these properties and the nature of wrapping of P3HT on CNT surfaces and its dispersion into TPU matrix were evaluated. Miscibility of the composite was ascertained from the single glass transition (T_g) ($\sim -40^{\circ}C$, obeying Fox equation) obtained through different thermal techniques (DMA, TMA).

EXPERIMENTAL

Materials

Commercial grade TPU was purchased from Bayer Materials, Germany under the trade name Desmopan (DP 9380A) and was used as a matrix without further purification. TPU is composed of poly(tetramethylene oxide) (PTMO), 2,4-diphenyl methylene diisocyanate (MDI), and 1,4-butanediol (BD). Regioregular poly(3-hexylthiophene) was purchased from Aldrich Chemicals, USA (mol wt = 45,000) and used without further purification. Material was kept in cold dark place before use. Short, thin multiwalled carbon nanotubes (MWNTs) were synthesized (NST Division, DMSRDE, Kanpur; purity, >85%; diameter 100 nm; length 1–1.5 μm)[25] by chemical vapor deposition process (Raman and SEM spectra in Supporting Information) and directly used in all the composites. Solvents (anhydrous tetrahydrofuran [THF], methanol. etc., Aldrich Chemicals, USA) were used after drying and purifying, following standard procedures.

Preparation of Composite

P3HT–TPU Blends. TPU was used as the base matrix and rrP3HT was embedded into it by mixing the solution of each component in THF.[26] At first, simple TPU was stirred in THF (40 mL) for 2 h and then rrP3HT was mixed into the solution under stirring for 6 h in inert atmosphere to produce the homogeneous mixture. Three casting solutions of P3HT/TPU (0.5, 2.5, and 5 wt % of P3HT in TPU) were prepared by mixing appropriate amount of P3HT into TPU solution. Films were prepared by solution casting method and dried under vacuum at room temperature for more than 1 week in inert atmosphere. Typical thickness of these films was of the order of 220 μm.

Ternary CNT–Nanocomposites. A given amount of rrP3HT (0.5, 2.5, and 5 wt %) and CNT (0.5 wt %) was sonicated using probe sonicator for 1 h 30 min in THF solution under inert atmosphere. Mechanical energy provided during sonication overcomes the Van der Waals interaction in the NT bundles, leading to NT exfoliation and at the same time rrP3HT molecules are adsorbed or wrapped onto the surface of NT walls. This rrP3HT-wrapped NT solution can be easily dispersed into TPU solution. The resulting mixture is further stirred for 5 h under inert atmosphere to get a stable dispersion with minimal nanotube aggregation. Films are formed by casting the blend solution and drying under vacuum at room temperature for more than 1 week. Thickness of the films is of the order of 400 μm. Compositions and sample codes used in this investigation are presented in table below:

Sample code	wt % of P3HT	wt % of MWNT
PH1	0.5	0
PH2	2.5	0
PH3	5.0	0
PHC1	0.5	0.5
PHC2	2.5	0.5
PHC3	5.0	0.5

Instrumentation

Thermal stability of the composite was measured using TGA 2950 TA instruments under nitrogen atmosphere. Samples were

heated at a scan rate of 10°C/min from room temperature to 600°C.

The melting point and enthalpy of composites were measured by differential scanning calorimetry (DSC) (TA instrument, model 2910). The instrument was calibrated with indium before each set of experiments. Samples were taken in Al pan and are crimped by Universal crimper. Samples were scanned at heating rate of 10°C/min from −100 to 250°C.

The tensile testing is carried out with an Instron Universal testing machine (model 100). The film samples are cut into size required for ASTM D 882 and the experiments are carried out at a crosshead speed of 50 mm/min at room temperature.

Dynamic mechanical properties of the composites were measured by using DMA (TA instrument 2980). Film dimension of 30 mm × 10 mm × 44 mm was made from the composite and then installed in the tension clamp of the calibrated instrument. Samples were heated from −130 to 100°C at a heating rate of 5°C/min. Storage modulus, loss modulus, and tan δ were measured at a constant frequency of 10 Hz with a static force of 0.5 N.

Glass transition temperature and coefficient of thermal expansion (CTE) were measured by TMA (TA instrument, model 2940) in an expansion probe mode. Each sample was heated from −100 to 200°C at a heating rate of 10°C/min. CTE of these composites was also measured in penetration probe mode at higher temperature.

RESULTS AND DISCUSSION

Stability of Blends and Nanocomposites

Controlled loading of rrP3HT (0.5–5 wt %) into THF solution of host matrix leads to a homogeneous mixture and evaporation of solvent results in the formation of a self-sustained homogeneous flexible blend. Fine dispersion of a small amount of CNT (0.5 wt %) into these solutions further enhanced the homogeneity of nanocomposites. Preferential wrapping of conducting polymers on CNT surface renders the wrapped CNT soluble in the host matrix's solution. Characterization of these samples demonstrates that 2.5 wt % of rrP3HT is ideal to wrap the entire surface of the CNT (0.5 wt %) uniformly and the highest molecular order, crystallinity, and crystal size are obtained in this ratio; lowering of rrP3HT amount (0.5 wt %) produces nonuniform wrapping, whereas excess loading (5 wt %) leads to agglomeration of P3HT.[27] Strong interaction between CNT and conducting polymer disturbs the self-organization of pristine rrP3HT and induces a new structural alignment of rrP3HT in the direction of CNT chain making the wrapped polymer too stable to precipitate out at all even after a weak methanol treatment.[27,28] It appears that modified self-assembly of conducting polymer in CNT–composites minimized the interfacial surface area of the aggregates exposed to poor solvent and thereby hindered its easy precipitation. Also, the prepared materials possess the typical magenta color characteristic of polymer molecule rod conformation in poor solvent.[27,29]

Spectral Characterization, Morphology, and Crystallinity

SEM images of TPU–rrP3HT blends indicate smooth homogeneous surface at low loading of P3HT (0.5 wt % loading of P3HT) and globular aggregates of P3HT dispersed uniformly all over the blend on increasing the P3HT loading (2.5 and 5 wt % loading of P3HT). No separate phase domain of P3HT is, however, observed in any of the above matrix and this is an excellent improvement with respect to blend homogeneity compared to earlier result where a heterophase blend with separate microdomain of P3HT is reported.[30] Fine dispersion of CNT in TPU–rrP3HT blends considerably reduces the aggregate size of P3HT globule in 5 wt % loaded P3HT nanocomposites, whereas in low-loaded P3HT (up to 2.5 wt %) globular aggregates of P3HT are virtually disappeared (Supporting Information).

Preferential wrapping of P3HT to the wall of MWNT do occur owing to π–π and CH–π interaction between the conjugated double bond of graphite ring and the conjugated double bond of P3HT.[31,32] A higher shift ($\sim$ 7–15 cm^{-1}) of CH-stretching (aliphatic) frequency region ($\sim$ 2925–2940 cm^{-1}) of P3HT suggests the presence of CH–π interaction. The presence of π–π interaction between thiophene ring of P3HT and graphite unit of MWNT is demonstrated by taking the antisymmetric C=C stretching (1505 cm^{-1}) and symmetric stretching (1457 cm^{-1}) vibration of thiophene ring.[30] In the composites, 1505 cm^{-1} peak is either obscured or not observed at all and also the frequency of the 1457 cm^{-1} peak decreases in intensity and downfield shifted in position by $\sim$ 7–17 cm^{-1} (Supporting Information).

The intensity ratio between antisymmetric (1505 cm^{-1}) and symmetric (1457 cm^{-1}) C=C stretching peak is used to probe the average conjugation length of P3HT in the composite at different P3HT loadings.[27,28,33,34] Conjugation length of P3HT polymer segments on the CNT surface depends on wrapping thickness of polymer and more uniform is the wrapping higher is intensity ratio and consequently higher is the conjugation length. The ratio is increased up to 2.5 wt % loading of P3HT and then it drops down on further increase of P3HT content. Highest intensity ratio at 2.5 wt % of P3HT loading is attributed to uniform thickest wrapping and maximum chain alignment of P3HT in the CNT–nanocomposites. Possibility of agglomeration considerably reduces the conjugation length of P3HT on 5 wt % loading of P3HT and accordingly intensity ratio reaches to its lowest value (Supporting Information).

P3HT–TPU and P3HT–TPU–MWNT composites' bulk structure is investigated by wide-angle X-ray diffraction technique and percentage crystallinity, crystal size, in-plane, and interplane distance of thiophene are calculated on the basis of X-ray diffraction data. In-plane interchain distance ($\sim$ 16.9 Å) and interplane π-staking distance (4.29 Å) of P3HT are increased in PHCs compared to PHs owing to unfolding of P3HT chain on wrapping on to CNT (Supporting Information). This study suggests that an optimum of 2.5 wt % of rrP3HT in 0.5 wt % of MWNT is an ideal ratio to be used as filler to obtain highest molecular order, crystallinity, and lower crystal size in CNT nanocomposite. A detail discussion on morphology, spectral characterization, and crystallinity of binary TPU/rrP3HT blends and that of ternary TPU/rrP3HT/CNT nanocomposites has been reported previously.[27]

Thermal Properties: TGA and DSC Analysis

TGA traces and first derivative TGA thermograms (heating rate 10°C/min in N_2-atmosphere) of PHs and PHCs are shown in

Applied Polymer SCIENCE

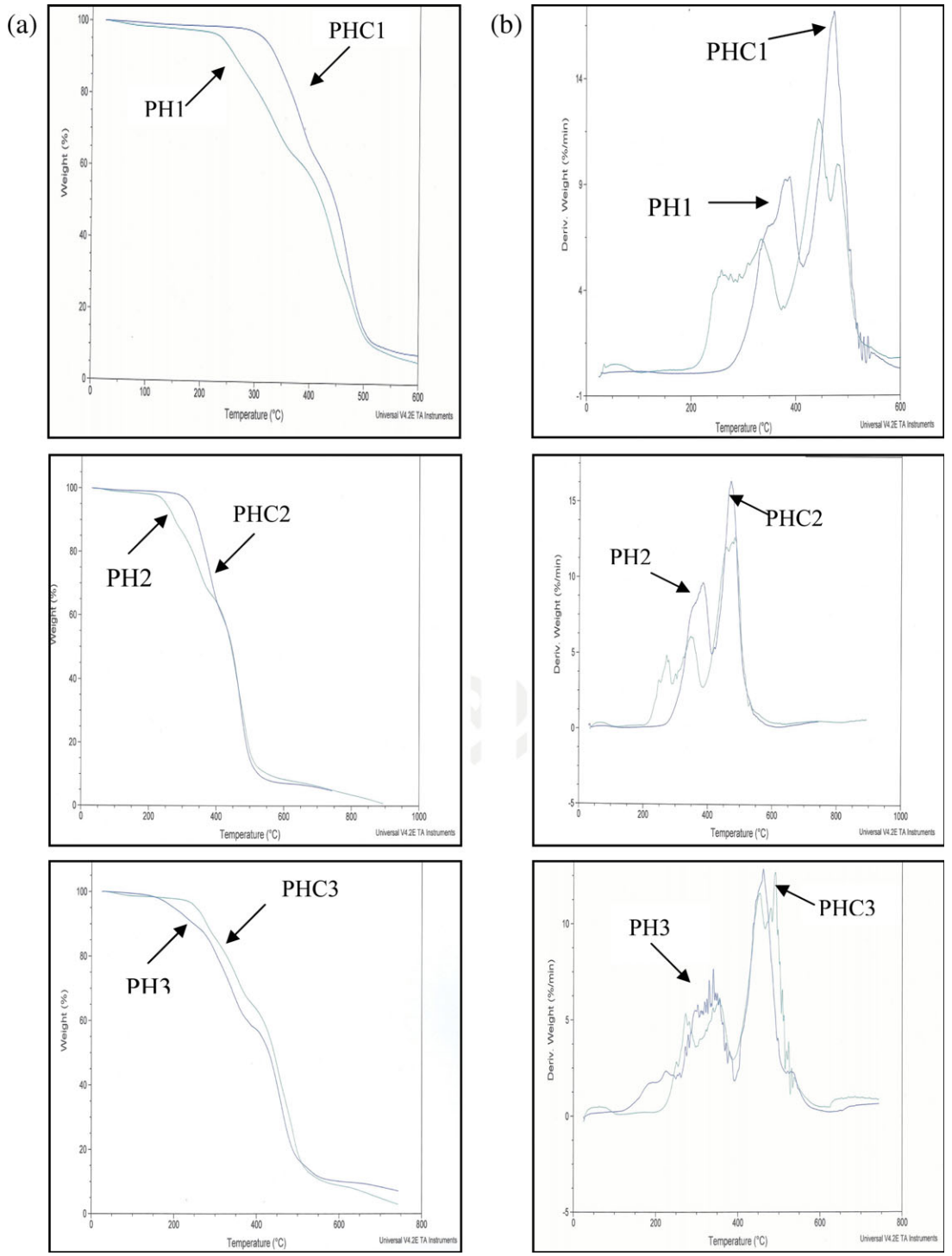

Figure 1. Comparative thermograms of PHs and PHCS: (a) TGA and (b) DTGA. [Color figure can be viewed in the online issue, which is available at wileyonlinelibrary.com.]

Figure 1 and summary of thermal data is provided in Table I. Host polymer matrix (TPU) exhibits an onset degradation temperature (onset of inflection) at 253°C and two-step degradation owing to soft and hard segments (Table I). Onset degradation temperature is typically defined as the temperature at which the material starts degrading its original structure and recorded as the meeting point of extrapolated straight lines drawn through plateau and slope. Regioregular P3HT has an onset degradation temperature at 453°C and two-step degradation owing to sequential release of alkyl groups attached at the 3-position of each thiophene ring followed by degradation of the aromatic rings.[35] TPU–P3HT blends (viz., PH1, PH2, and PH3) show onset degradation temperatures at 234, 244, and 175°C, respectively. Three-step degradation was observed at

Table I. Summary of TG Data of TPU, CNT, rrP3HT, and Their Binary and Ternary Blends Recorded at a Heating Rate of 10°C/min in N_2-Atmosphere

Sample name	Onset of decomposition	Stepwise decomposition		
		Temperature	% wt loss	T_{max}
TPU	250	250-378	25	275
		250-378	74	432
P3HT	453	453-587	57	524
		587-840	42	727
MWNT	500	500-910	70	765
PH1	234	234-350	34	334
		350-416	15	444
		416-500	40	479
PH2	244	244-322	32	272
		322-430	25	347
		430-550	56	482
PH3	175	175-292	9	225
		292-428	32	340
		428-520	43	461
PHC1	328	328-449	38	388
		449-510	53	473
PHC2	328	328-448	38	384
		448-500	54	469
PHC3	251	251-330	20	273
		330-434	15	355
		434-500	56	491

relatively higher temperature in all the blends and the steps for sequential release of alkyl groups were more clearly visible (Table I). As summarized in Table I, blends show relatively lower thermal stability than that of pure TPU. Although the reason for lower thermal stability of the blends on addition of rrP3HT is not completely understood, one can plausibly argue from the nature of the trend in positioning of the degradation temperature that globular nature of rrP3HT forms defects on TPU matrix. Agglomeration of rrP3HT globules in higher concentration dramatically reduces the thermal stability of TPU matrix. More definite ordered arrangement of alkyl side chains of rrP3HT is, however, noted from more distinct steps for the release of alkyl side chain in differential thermogravimetric analysis (DTGA). Significant shift in onset degradation temperatures toward higher value was observed on addition of MWNT. The first mass loss step occurred at about 325°C for CNT nanocomposites and the second degradation step started at about 500°C. The first mass loss step is owing to the loss of an alkyl group attached to thiophene backbone (hexyl group) and also the loss of host polymer matrix. As the temperature increased above 500°C, oxidation accelerated and pyrolysis of the aromatic backbone of polymer chains was ignited. DTGA thermograms clearly show that cleavage of the hexyl group as well as the aromatic backbone occurs in two steps and the multiple overlapping steps for the release of hexyl groups in pristine rrP3HT at small temperature zone (all hexyl groups are thermally equivalent) are transformed into more definite steps owing to the alignment of P3HT on interaction with MWNT in composites (thermal equivalency of hexyl groups is disturbed). It is attributed that wrapping of P3HT on to the wall of MWNT (through π–π and CH–π interaction) might have overcome the globular defects structure of P3HT in matrix. This result indicates that MWNT acts as barriers to P3HT owing to their high aspect ratio and hinders the degradation process. Tight adsorption of aromatic backbones of P3HT onto thermally stable MWNT's surface through noncovalent interaction enhances thermo-oxidative stability of the composites. Multiple decomposition steps of both hexyl groups and thiophene backbone appear again at higher weight percent of P3HT loading (5 wt %) owing to reasonable excess amount of P3HT in composite.

The DSC study was carried out to elucidate the thermal properties of composites across melting and crystallization region. Semi-crystalline regioregular P3HT polymer can show two types of crystals, one of them is interdigitated (Figure 2).[36] Side-chain crystallization and the presence of a nematic mesophase in the liquid are proposed to occur depending on methods, materials, and measurement conditions used. Pristine rrP3HT shows a large melting region from 200 to 245°C with a melting peak at around 235°C [Figure 3(a)]. A very low heat of melting (ΔH_m = 16.66 J/g) is, however, observed in pure rrP3HT and is consistent with partial crystallinity and nematic mesophase expected to be present in liquid phase.[2] Matrix polymer (TPU) shows glass transition (T_g) at around −41°C (soft segment) and two melting temperatures (T_m); first one at around 166°C (soft segment) and other one at around 224°C (hard segment) [Figure 3(b)]. First heating curve of TPU–P3HT blends records significant shifting of soft segment melting peak toward higher region on increasing P3HT loading. Melting peaks are recorded at around 90, 92, and 103°C for PH1, PH2, and PH3, respectively. The exact reason for this increase in melting is unknown but it may be possible that there are some types of physical and/or chemical interaction between TPU and P3HT [Figure 3(c–e)].

Heat flow curves of first heating run (rate, 10°C/min) for nanocomposites are shown in Figure 4(a). Melting peak of

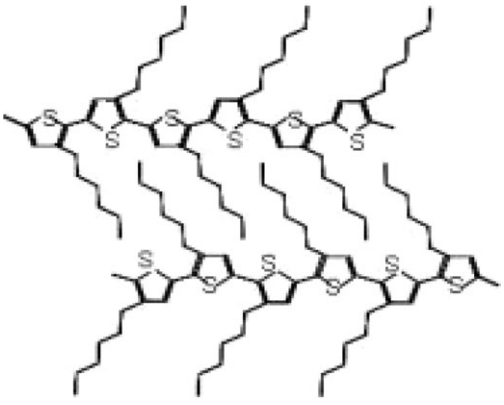

Figure 2. Schematic model of lamellar crystal of P3HT where polymer chain interdigitated with hexyl groups.

Applied Polymer SCIENCE

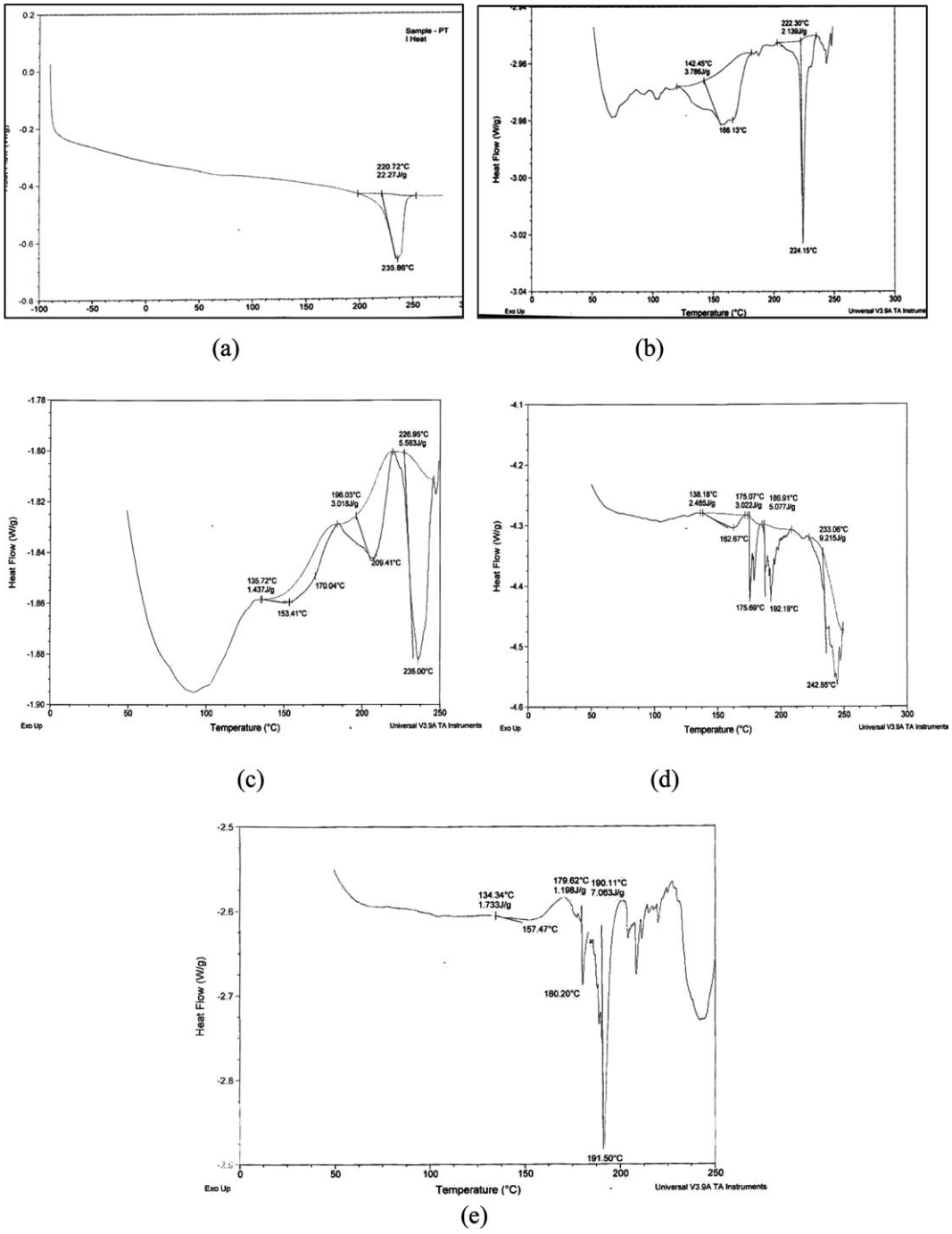

Figure 3. DSC thermograms at heating rate of 10°C/min under N_2: (a) P3HT, (b) TPU, (c)TPU + 0.5% P3HT, (d) TPU + 2.5% P3HT, and (e) TPU + 5.0% P3HT.

P3HT in PHC1 and PHC3 was observed at about 234 and 236°C, respectively, whereas in PHC2, the melting peak occurs at around 226°C. Heat of melting (ΔH_m) for PHC1, PHC2, and PHC3 were 11.87, 8.073, and 14.63 J/g, respectively, lower than that of pure rrP3HT. The lowest heat of melting value was recorded in the case of PHC2. It may be plausibly argued that uniform wrapping of rrP3HT on CNT surface leads to maximum uncoiling of P3HT structures in the direction of the CNT and thus forms a more homogenous system. Such homogenous nanocomposite systems require minimum heat of melting for rrP3HT. It is believed that owing to higher ratio of CNT in PHC1, more heating is required to melt the blend. On the other hand, higher amount of rrP3HT results globular domains in TPU matrix in PHC3 and requires higher energy input during "coil-to-rod transformation" of rrP3HT.

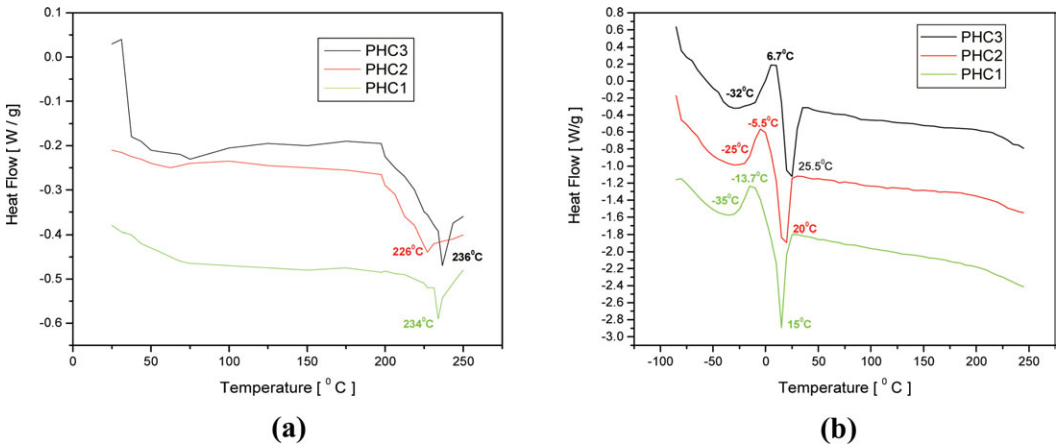

Figure 4. DSC thermograms of TPU–P3HT–CNT ternary system at heating rate of 10°C/min under N_2: (a) first heating run thermograms and (b) second heating run thermograms. [Color figure can be viewed in the online issue, which is available at wileyonlinelibrary.com.]

Interestingly, a distinctly different second heating run curve is observed in case of ternary systems. Heat flow curves of second heating run (rate, 10°C/min) for three nanocomposites (viz., PHC1, PHC2, and PHC3) do not show any distinct melting peak of P3HT at around 230°C [Figure 4(b)]. Instead, it shows a large endothermic melting region from −12.5 to 26.5°C having peak at ∼ 15°C for PHC1. Other ternary systems, viz., PHC2, on the other hand, records a endothermic melting region from −5 to 26.5°C with a peak at ∼ 20°C and PHC3 shows melting region from 8 to 35.5°C with a peak at ∼ 25.5°C. This melting region appears owing to side-chain melting and is not observed in first heating run curve. It is apparent from the crystallization data that unlike first heating curve, the second heating run curve bears a simple linear relationship between amount of P3HT loading and side-chain melting: higher the amount of P3HT loading, the higher is side-chain melting peak of P3HT in the composites. This increase is about 5°C for 2–2.5% increase of P3HT loading in the composites.

Also, T_g of TPU soft segment is shifted to a large extent in PHC2 (−25°C) compared to PHC1 (−32°C) and PHC3 (−35°C). This supports the fact that more homogeneously dispersed MWNT decreases the chain mobility of TPU matrix owing to its better interaction in uniformly wrapped P3HT (at 2.5 wt % of P3HT). In the cooling curve, a crystallization exothermic peak is observed at around −13.7, −5.5, and 6.7°C for PHC1, PHC2, and PHC3, respectively. It is probable that CH–π or π–π interaction in uniformly wrapped MWNT resists the tilting of the P3HT side chains and helps side chain to be more interdigitated, inducing more crystalline structure. Globule formation (at higher loading) and improper wrapping on CNT (at low loading of P3HT) does influence the side-chain crystallization of P3HT.

Mechanical Property: Stress–Strain Behavior

Mechanical properties of simple TPU, TPU–P3HT blend, and TPU–P3HT–MWNT composites are investigated. Typical stress–strain curves for TPU and composites containing 0.5, 2.5, and 5 wt % of P3HT are shown in Figures 5 and 6. All the composites show a nonlinear elastic behavior in the low stress region and upward rise of the curve before breaking point at higher stress region. It is attributed that chain alignment owing to stress-induced crystallization increases the stress at breaking point.[3,8] The maximum stress at break is tensile strength (TS). It is observed that pristine TPU has higher TS and tensile modulus compared to TPU–P3HT blend but has lower TS and tensile modulus (except 5 wt % of P3HT) compared to CNT-reinforced nanocomposites (Table II). Higher level of structural disorder of TPU matrix owing to intermolecular interaction at the interfaces on addition of P3HT leads to lowering of TS and tensile modulus. It is interesting to mention that this structural disorder on addition of P3HT enhances flexibility of TPU resulting in approximately five to six times higher elongation. Addition of MWNT in the TPU–P3HT system increases TS and tensile modulus; highest T.S and modulus is exhibited in TPU–P3HT system containing 2.5 wt %-loaded P3HT. It is more probable that uniformly P3HT-wrapped CNT is well dispersed in TPU matrix compared to other composite systems where the aggregation or improper wrapping of P3HT on CNT (Supporting Information, FTIR and XRD analysis) causes defect structure. Results also indicate that using MWNT as a reinforcing

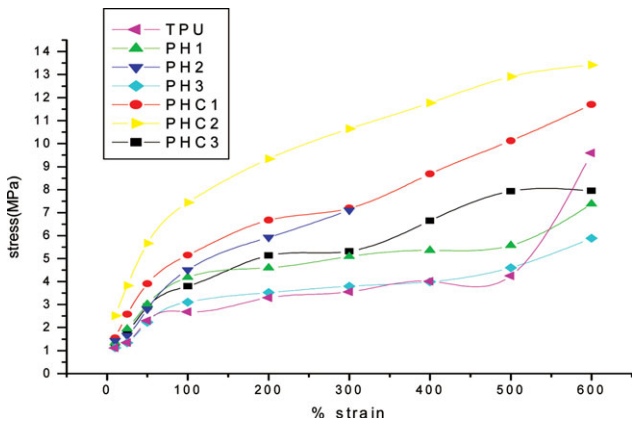

Figure 5. Stress–strain behavior of pristine TPU, PHs, and PHCs. [Color figure can be viewed in the online issue, which is available at wileyonlinelibrary.com.]

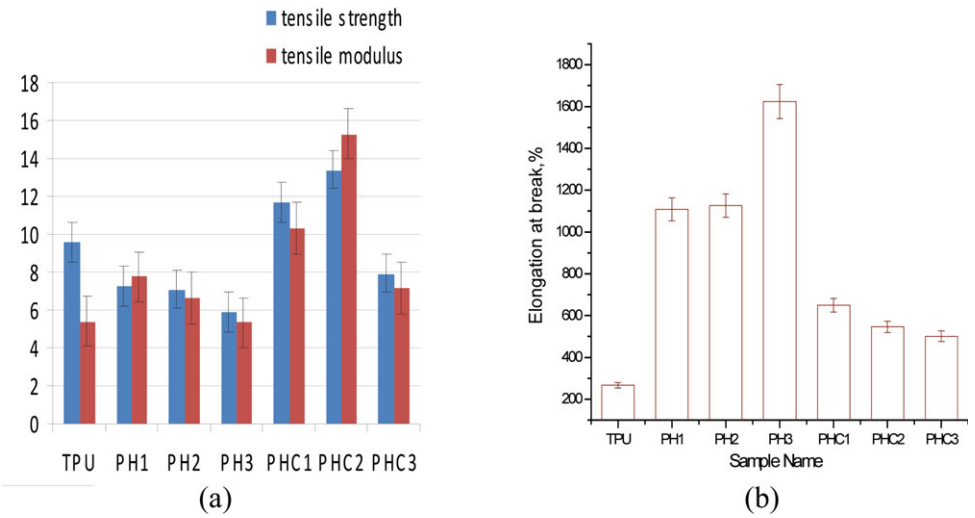

Figure 6. Variation of (a) TS and tensile modulus, (b) percentage elongation at break in PHs and PHCs with increasing weight percent of P3HT. [Color figure can be viewed in the online issue, which is available at wileyonlinelibrary.com.]

agent resistance against mechanical deformation can be improved without sacrificing the original elongation at break of simple TPU.

Dynamic Mechanical Analysis

Dynamic mechanical thermal analysis (DMA) was performed to evaluate the variation of storage modulus (E'), loss modulus (E''), and tan δ with respect to temperature for binary and ternary composites at different wt % of P3HT. Comparative DMA thermograms of TPU–P3HT blends and effects on addition of MWNT in nanocomposites are shown in Figure 7 and the data are summarized in Table III. Storage modulus or elastic modulus (E') represents the ability of the material to store or retain mechanical energy when an oscillatory force is applied to the sample and it is the quantitative measure of the stiffness or rigidity of the material. Extrapolated onset temperature of storage modulus defines the temperature at which the material's strength will begin to decrease so that the material will no longer be able to bear a load without deformation. Extrapolated onset temperature of storage modulus is reported as T_g of the material.[26,37] Loss modulus (E'') relates the ability of the material to dissipate the mechanical energy by converting it into heat. Tan δ is the ratio of loss modulus to storage modulus and tan δ_{max} value indicates the damping characteristics of the material. Loss modulus and tan δ plots are two different modes of measurement; one is related to the dissipation of energy as heat (loss modulus), and the other is related to the reduction of vibration of the material, that is, damping (tan δ). It is possible to have difference in transition temperatures obtained from loss modulus and tan δ plots owing to two different modes of measurement.

Generally, commercial grade TPU (Desmopan [DP 9380 A]) has large difference between glassy modulus (E_g) and rubbery modulus (E_r) ratio, conducive for fast shape recovery properties. Glassy modulus is owing to the presence of elastic energy of both PTMO and urethane phase and rubbery modulus is owing to the entropy of elasticity of the two-phase structure of the material.[26,37] Increase in hard segments (acting as a physical crosslinks) owing to a higher proportion of BD and MDI units in PUs raise the glassy modulus. It is seen that increase in hard segment content leads to higher E_g and lower E_r, resulting in large modulus ratio conducive for a better shape recovery property. Higher loss tangent value indicates that the material tends to be more viscous. Large difference in modulus below and above the transition temperature and sharp glass–rubber transition is the most essential requirement to render shape memory function. With phase-separated structure, hard segment acts as a physical crosslink and effectively reinforces the soft segments in the rubbery state.

From DMA thermograms, it is apparent that increase in temperature decreases storage modulus and it is negligibly small at about 50°C for all samples [Figure 7(a)]. Storage modulus of TPU–P3HT blends is lower than that of pure TPU. Intermolecular interaction at the interphase between TPU and P3HT leads to an enhancement of structural disorder of the soft segment of TPU matrix and may possibly be responsible for lowering of the storage modulus. This structural disorder favors the chain flexibility of P3HT in TPU matrix. More structural disorder occurring owing to increase of P3HT causes further lowering of the

Table II. Mechanical Properties of PHs and PHCs With Varying wt % of P3HT

Sample name	TS	Tensile modulus	% Elongation at break
TPU	9.59	8.39	267.2
PH1	7.28	7.75	1108.5
PH2	7.11	6.64	1126.5
PH3	5.89	5.34	1623.9
PHC1	11.70	10.33	648.2
PHC2	13.41	15.29	546.1
PHC3	7.95	7.14	510.5

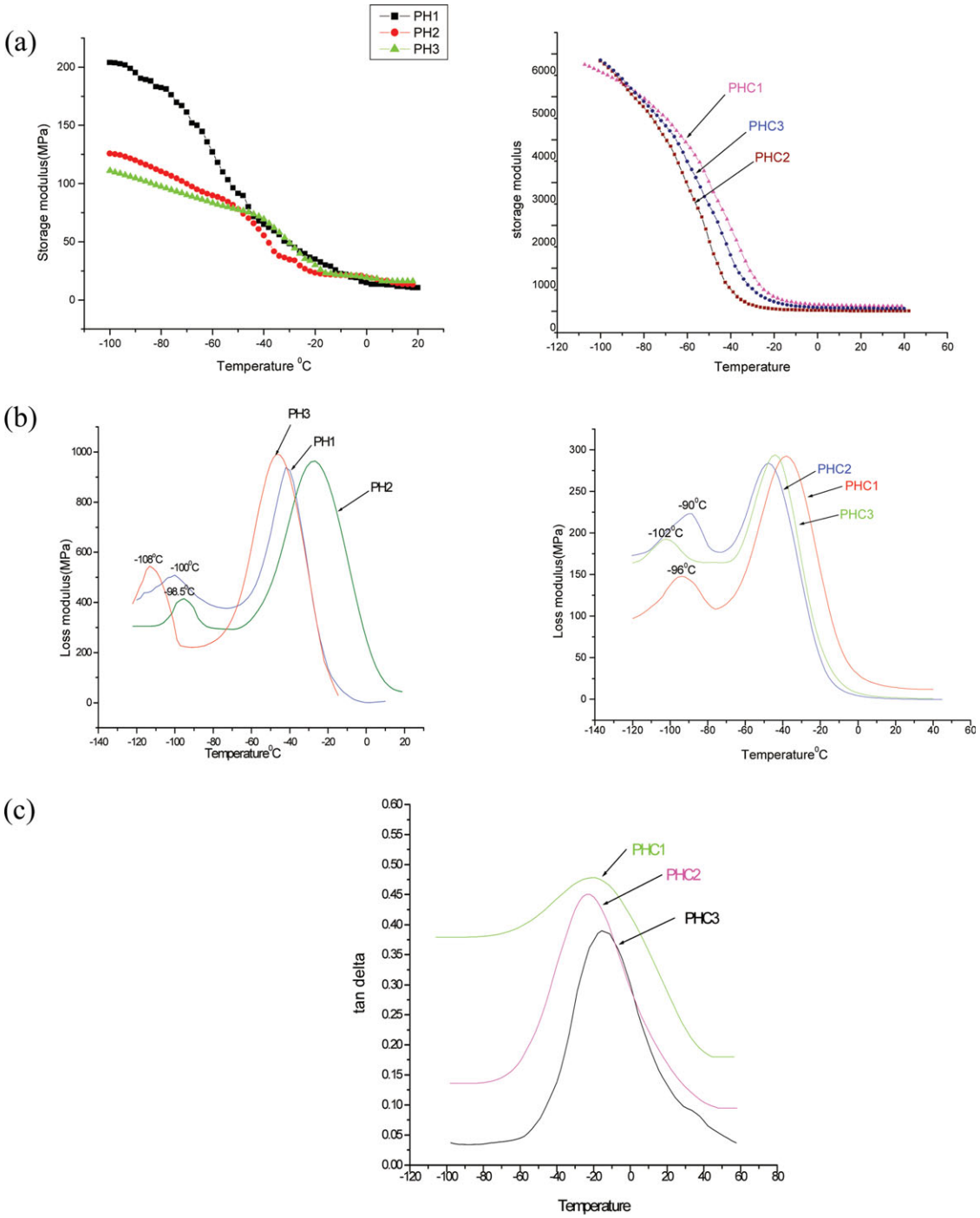

Figure 7. Variation of mechanical property with temperature. (a) Storage modulus, (b) loss modulus, and (c) tan δ studied in DMA mode. [Color figure can be viewed in the online issue, which is available at wileyonlinelibrary.com.]

storage modulus. The presence of CNT, on the other hand, enhances large mechanical reinforcement in nanocomposites owing to large surface area and high aspect ratio and improves storage modulus (Figure 7(a) and Table III). Mechanical reinforcement is higher below T_g compared to those at 20°C. Wrapping of CNT with P3HT through CH–π and π–π interaction allows homogeneous dispersion of wrapped CNT in TPU matrix and chain mobility of polyurethane is more restricted below T_g. These restrictions are negligible above T_g when all segmental motions such as side- and main-chain motion are already started. Storage modulus is lower at 5 wt % of P3HT loading compared to PHC1 and PHC2 owing to improper wrapping and nonuniform dispersion of wrapped CNT in TPU. Loss modulus vs. temperature plots show two break points for both PHs and PHCs, one at lower temperature (~ -100°C) and other at higher temperature (~ -40°C) [Figure 7(b)],

Table III. Summary of Mechanical Properties of PHs and PHCs Measured by DMA

Sample name	T_β (°C)	T_g (°C)	Storage modulus (MPa)	
			−50°C	20°C
TPU	-	−41.45	580	10
PH1	−100	−40	85	18
PH2	−98.5	−34	80	25
PH3	−110	−48	75	25
PHC1	−96	−40	2400	600
PHC2	−90	−50	2700	500
PHC3	−102	−46	2000	800

indicating two different types of transitions in the P3HT chains. The peak at lower temperature (T_β) arises from the relaxation of hexyl side chains (β-transition), whereas the peak at higher temperature arises from the relaxation of main chains (α-transition). This α-transition temperature is also called as the glass transition temperature (T_g) of the material. It is very interesting to mention here that both PH and PHC systems record a single T_g, confirming homogeneity during their formation (Figure 7 and Table III). An increase in T_g is, however, observed for PH2 and the actual reason is not known. As summarized in Table III, it is observed that T_β exhibits abnormally higher value in PHCs than that of PHs. This indicates that the wrapping of P3HT on CNT hinders the hexyl group's bond rotation relaxation pathway. T_β is not changed so remarkably in PHs except PH3 compared to pristine P3HT (−100°C). Improper wrapping on CNT in PHC3 also causes lowering of T_β compared to PHC1 and PHC2.

Thermomechanical Analysis

Thermomechanical analyses (TMAs) give an idea about T_g and dimensional stability of samples at a low loading condition. Low-temperature dimensional stability of both PH and PHC samples is measured using the expansion probe technique. In the expansion probe technique, the probe is rested on the surface of the test specimen at very low loading condition and as the sample expands during heating, the probe is pushed up and

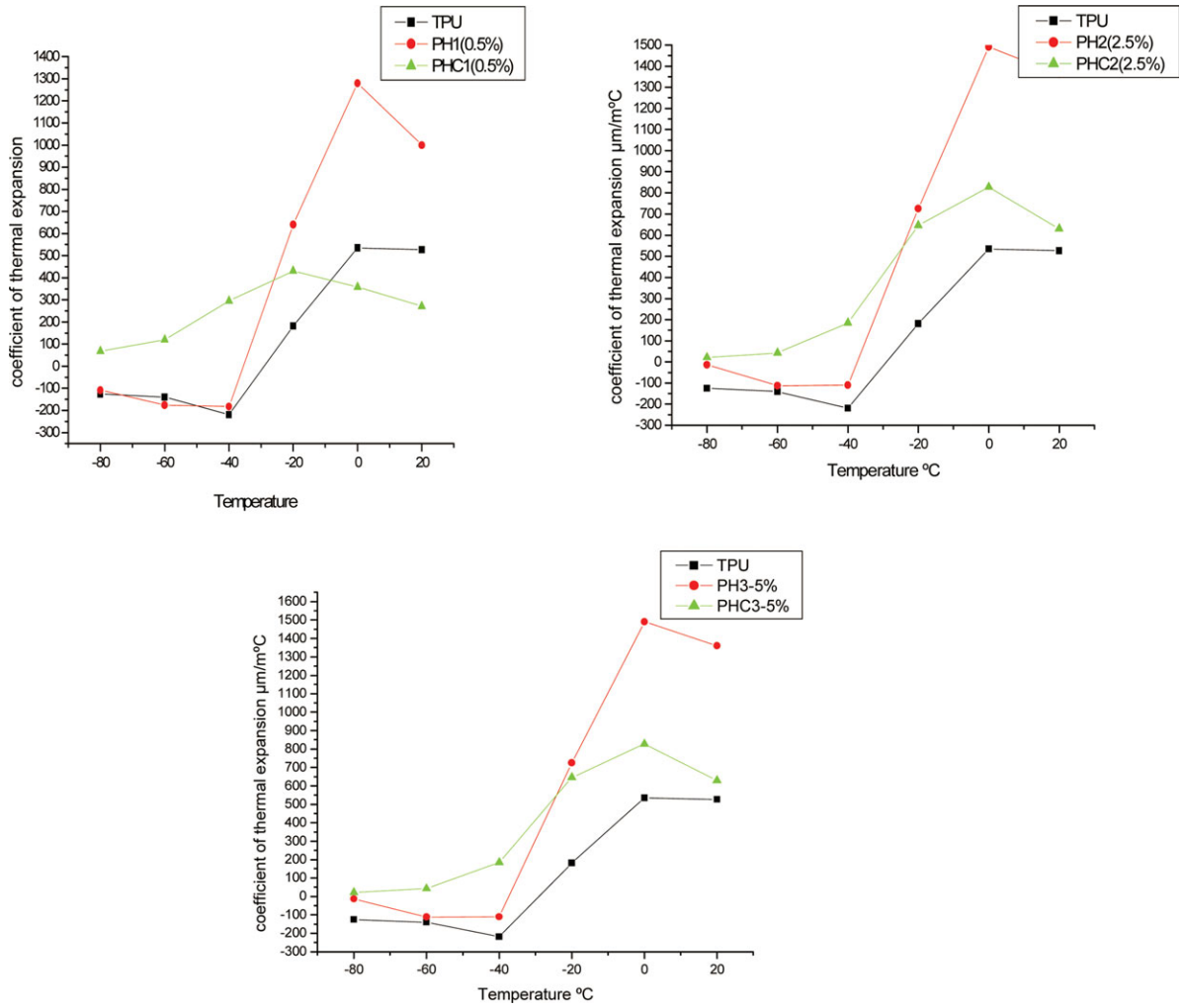

Figure 8. TMA thermograms for the variation of CTE and T_g of PHs and PHCs using expansion probe. [Color figure can be viewed in the online issue, which is available at wileyonlinelibrary.com.]

Table IV. Summary of TMA Thermogram Data of TPU–P3HT Blend Using Expansion Probe

Sample name	Max. rate of expansion (μm/min)	% Expansion	Max. rate of contraction (μm/min)	% Contraction
TPU	6.9	7.3	48.6	29.7
PH1	5.98	5.70	1.09	0.99
PH2	7.74	7.11	0.27	0.16
PH3	6.42	7.01	0.66	0.47
PHC1	5.11	3.06	0.64	0.84
PHC2	4.67	2.73	0.47	0.18
PHC3	5.16	4.22	0.44	0.51

the resulting expansion of the sample is measured. Basically, this change in dimension is owing to the activation of molecules. An increased thermal vibration produces thermal expansion owing to the activation of molecules and is characterized by the CTE. In expansion probe TMA technique, the variation of CTE is recorded at a controlled rate of heat change. CTE is defined as the rate of change of dimension per degree rise of temperature/per unit time. The particular temperature at which sudden rise in the CTE occurs owing to significant loss of dimension stability manifested by an extraordinary increase of expansion probe is called T_g. T_g is basically measured as a tangent (slope) obtained from the meeting points of the two extrapolated lines of CTE vs. temperature graph as shown in Figure 8. It is illustrated that CTE is low at glassy state where the degree of molecular segmental motion is restricted. At T_g, the degree of molecular segmental motion becomes increasing very fast and consequently, CTE is high at the rubbery state. From CTE vs. temperature graph (Figure 8), it is also seen that T_g of TPU is shifted from −29 to −40°C on blending with P3HT and a single T_g is observed in each blend composition. Appearance of a single T_g confirms homogeneity of blends. The experimental T_g values are in good agreement with T_g obtained from other techniques and also calculated using Fox equation. T_g-values virtually remained unchanged on addition of CNT except for PHC1 (Figure 8). This slight exception observed in PHC1 may plausibly be explained by the fact that although incorporation of CNT increases the T_g of TPU, there is an opposing effect

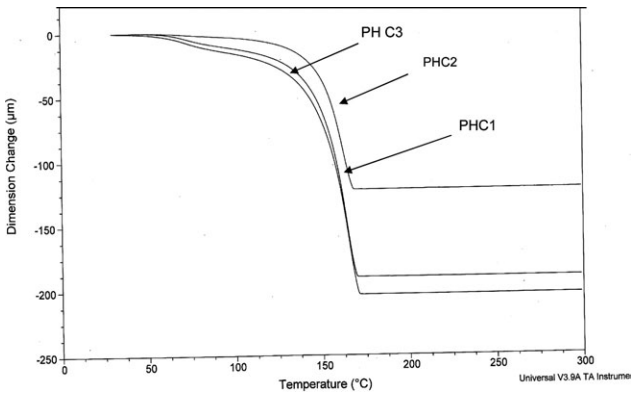

Figure 9. TMA thermograms of PHCs using penetration probe.

Table V. Summary of TMA Thermogram Data of PHCs Using Penetration Probe

Sample name	Max. rate of expansion (μm/min)	% Expansion	Max. rate of penetration (μm/min)	% Penetration
PHC1	5.11	3.06	64.11	53.36
PHC2	4.67	2.73	64.58	62.98
PHC3	5.17	4.22	92.10	48.23

caused by P3HT. P3HT is a semi-crystalline polymer and crystalline regions are interspersed with amorphous regions. These closely associated amorphous regions have lower degree of freedom than the bulk amorphous phase and are expected to lower the CTE value on addition of this rigid amorphous P3HT into the TPU matrix. The CTE value increases significantly (compared to pristine TPU) on increasing P3HT loading (above 0.5 wt %). Intermolecular interaction at the interphase between TPU and P3HT clearly disturbs the structural ordering of soft segment of TPU to enhance chain mobility and thus enhances the CTE value. Thus, wide variation of CTE between pristine TPU and PHs may build up uneven thermal stresses during operation. Addition of MWNT (0.5 wt %) in TPU–P3HT blend amicably solves both structural and crystal reorganization problems of P3HT. The thermally activated process of wrapping of P3HT on CNT unfolds the P3HT main chain to interfere with TPU during thermal expansion process. Further, all the TPU–P3HT blends have higher rate of expansion and contraction compared to PHC nanocomposites which have no contraction at lower temperature (Table IV). Dimensional stability is also measured above ambient temperature under penetration probe for PHC nanocomposites (Figure 9 and Table V). Penetration probe measurement is performed with added load to the probe so that it moves down as the material becomes soften. Penetration probe technique provides excellent idea about the softening properties of materials during normal usage condition. It is interesting to mention here that the nanocomposite in which P3HT-wrapped MWNT is uniformly dispersed in TPU (PHC2; 2.5 wt % loading of P3HT) exhibits lowest degree of penetration. Other composites (viz., PHC1 and PHC3) where CNT is not uniformly dispersed owing to improper wrapping show lower restriction to probe penetration, resulting higher rate of penetration.

CONCLUSIONS

The above studies establish an excellent correlation of the effect of dispersion of P3HT-wrapped CNT on dynamic and thermomechanical properties of P3HT–TPU–CNT ternary nanocomposites and its comparison with P3HT–TPU blends. Wrapping of P3HT on CNT makes the hexyl side groups thermally nonequivalent and also makes the composites more stable. The DMA study indicates lowering of storage modulus and enhancement of chain flexibility for TPU–P3HT blends compared to pure TPU, owing to structural disorder of the soft segment of TPU matrix and this has direct relationship with the amount of P3HT loading; increased loading of P3HT causes further

lowering of storage modulus. The presence of CNT, on the other hand, influences a large mechanical reinforcement in PHC nanocomposites and improves the storage modulus. Loss modulus vs. temperature plots show two breaks in all the PH and PHC samples; the first one at lower temperature ($\sim -100°C$) and the other at higher temperature ($\sim -40°C$), indicating two different types of transitions in the P3HT chains. The lower temperature peak (T_β) arises from the β-transition (i.e., relaxation of hexyl side chains) and higher temperature peak arise from the α-transition (i.e., relaxation of main chain); also called T_g of the material. Both PHs and PHCs have a single T_g, confirming homogeneity during blend formation.

Dimensional stability of the PHC samples measured using expansion probe illustrates that the CTE is low at glassy state and high at the rubbery state compared to PH samples. CTE vs. temperature graph also shows that T_g of TPU is shifted from -29 to $-40°C$ on blending with P3HT and a single T_g is observed in each blend composition. These experimental T_g values are in good agreement with other measurement techniques and also calculated using Fox equation. TPU–P3HT blends have higher rate of expansion and contraction compared to PHC nanocomposites. Softening properties of materials, measured by penetration probe technique, suggest that uniformly P3HT-wrapped MWNT (PHC2; 2.5 wt % loading of P3HT) exhibit lowest degree of penetration compared to other nanocomposites.

REFERENCES

1. Njuguna, J.; Pielichowski. K. *J. Mater. Sci.* **2004,** *39*, 4081.
2. Patrıcio, P. S. O.; Calado, H. D. R.; de Oliveira, F. A. C.; Bernardo, A. R.; Neves, R. A.; Silva, G. G.; Cury. L. A. *J. Phys. Condens. Matter* **2006,** *18*, 7529.
3. Chen, W.; Tao, X.; Liu, Y. *Comp. Sci. Tech.* **2006,** *66*, 3029.
4. Merline, J. D.; Nair, C. P. R.; Gouri, C.; Ninan, K. N. *J. Appl. Polym. Sci.* **2008,** *107*, 4082.
5. Kim, B. K.; Lee, S. Y. *Polymer* **1996,** *37*, 5781.
6. Wang, F.; Gu, H.; Swager, T. M. *J. Am. Chem. Soc.* **2008,** *130*, 5392.
7. Hatchett, D. W.; Josowicz, M. *Chem. Rev.* **2008,** *108*, 746.
8. Ruckenstein, E.; Sun, Y. *Synth. Met.* **1995,** *75*, 79.
9. Shirakawa, H.; Louis, E. J.; MacDiarmid, A. G.; Chiang, C. H. Heeger, A. J.; *J. Chem. Soc. Chem. Commun.* **1977,** *16*, 578.
10. Star, A.; Lu, Y.; Bradley, K. G. *Nano Lett.* **2004,** *4*, 1587.
11. Osaka, I.; McCullough, R. D. *Acc. Chem. Res.* **2008,** *41*, 1202.
12. McCullough, R. D.; Lowe, R. D. *J. Chem. Soc. Chem. Commun.* **1992,** *1*, 70.
13. Chen, T. A.; Rieke, R. D. *Chem. Rev.* **1992,** *92*, 711.
14. Wu, X.; Chen, T. A.; Rieke, R. D. *Macromoleucles* **1996,** *29*, 7671.
15. Skotheim, T. A.; Elsenbaumer, R. L.; Renolds, J. R. Handbook of Conducting Polymer, 2nd ed.; M. Dekker: New York, **1998, p 225.**
16. Pal, S.; Roy, S.; Nandi, A. K. *J. Phys. Chem. B* **2005,** *109*, 18332.
17. Kabashi, M.; Takeuchi, H. *Macromolecules* **1998,** *31*, 7273.
18. McCarthy, B.; Coleman, J. N.; Czerw, R.; Dalton, A. B.; Maiti, A.; Drury, A.; Bernier, P.; Nagy, J. B.; Lahr, B. H. J.; Carroll, D. L.; Blau, W. J. *J. Phys. Chem. B* **2002,** *106*, 2210.
19. Haddon, R. C. *Special Issue: Carbon Nanotubes. Acc. Chem. Res.* **2002,** *35*, 997.
20. Ajayan, P. M. *Chem. Rev.* **1999,** *99*, 1787.
21. Tang, B. Z.; Xu, H. *Macromolecules* **1999,** *32*, 2569.
22. Zhang, R.; Dowden, A.; Deng, H.; Baxendale, M.; Pejis, T. *Comp. Sci. Tech.* **2009,** *69*, 1499.
23. Song, Y. J.; Lee, J. U.; Jo, W. H. *Carbon* **2010,** *48*, 389.
24. Kuila, B. K.; Malik, S.; Batabyal, S. K.; Nandi, A. K. *Macromolecules* **2007,** *40*, 278.
25. Roy, D.; Tripathi, N. K.; Saraiya, A.; Ram, K. *Synth. Met.* **2009,** *159*, 434.
26. Grossiord, N.; Loos, J.; Regev, O.; Koning, C. E. *Chem. Mater.* **2006,** *18*, 1089.
27. Saha, S.; Singh, J. P.; Saha, U.; Goswami, T. H. Rao, K. U. B. *Comp. Sci. Tech.* **2011,** *71*, 397.
28. Musumeci, A. W.; Silva, G. G.; Liu, J. W.; Martens, W. N.; Waclawik, E. R. *Polymer* **2007,** *48*, 1667.
29. Rughooputh, S. D. D. V.; Hotta, S.; Heeger, A. J.; Wudl, F. J. *J. Polym. Sci. B Polym. Phys.* **1987,** *25*, 1071.
30. Chen, T. A.; Wu, X.; Rieke, R. D. *J. Am. Chem. Soc.* **1995,** *117*, 233.
31. Kymakis, E.; Amaratunga, G. A. *J. Synth. Met.* **2004,** *142*, 161.
32. Bhaskaran, D.; Mays, J. W.; Bratcher, M. S. *Chem. Mater.* **2005,** *17*, 3389.
33. Furukawa, Y.; Akimoto, M.; Harada, I. *Synth Met* **1987,** *18*, 151.
34. Trznadel, M.; Pron, A.; Zagorska, M.; Chrzaszcz, R.; Pielichowski, J. *Macromolecules* **1998,** *31*, 5051.
35. Adhikari, A. R.; Huang, M.; Bakhru, H.; Chipara, M.; Ryu, C. Y.; Ajayan, P. M. *Nanotechnology* **2006,** *17*, 5947.
36. Prosa, T. J.; Winokur, M. J.; McCullough, R. D. *Macromolecules* **1996,** *29*, 3654.
37. Schwartz, B. J. *Ann. Rev. Phys. Chem.* **2003,** *54*, 141.